RSC Advances

PAPER

View Article Online
View Journal | View Issue

Cite this: *RSC Adv.*, 2017, **7**, 34816

Theoretical insights into C–C bond formation through isonitrile insertion into a Cp*Ti complex†

Ming-Ran Du,‡[a] Xiang-Biao Zhang,*[a] Sheng-Meng Si,‡[a] Feng Yang‡[a] and Lei Wang*[b]

Received 19th May 2017
Accepted 6th July 2017

DOI: 10.1039/c7ra05680j

rsc.li/rsc-advances

The migratory insertion of isonitriles into the metal–C bond is important for constructing C–C bonds in organic and pharmaceutical syntheses. We examine the reaction of Cp*(Cl)Ti(diene) with isonitriles using density functional theory calculations. At room temperature, the bis-insertion reaction occurs easily for *N*-*tert*-butyl (*t*Bu), methyl (Me), ethyl (Et), 2,6-dimethylphenyl (Ar), and *N*-1-adamantyl (1-Ad)-substituted isonitriles. The elementary reactions include the isomerisation of Cp*(Cl)Ti(diene), migratory insertion of the first isonitrile into a Ti–C bond, C–C reductive elimination, β-H elimination, migratory insertion of the second isonitrile into a Ti–H bond, and C–C reductive coupling. Two reliable fragmentation mechanisms are suggested for the bis-insertion products. For the bulkier *t*BuNC, ArNC, and 1-AdNC, the β-H elimination reaction pathway is dominant. For the smaller MeNC and EtNC, the γ-H elimination reaction pathway competes with the β-H elimination. For ArNC, the isomerisation reaction pathway to a newly predicted "σ complex" is kinetically favourable.

Introduction

Ti complexes have displayed powerful and tunable reactivities, in addition to other advantages such as the abundance of Ti in the earth and its low toxicity and cost.[1–11] Tonks *et al.* reported the $[py_2TiCl_2NPh]_2$-catalysed synthesis of α,β-unsaturated imines and α-(iminomethyl)cyclopropanes through multi-component reactions, which couple alkynes, alkenes, and diazenes and show substrate control selectivity.[1d] Xie *et al.* developed a methodology for the efficient synthesis of mono/bicyclic guanidines catalysed by a Ti-amide, and obtained chiral guanidines.[2c] Xia and Li *et al.* described an efficient method to synthesise substituted piperazines through $Ti(NMe_2)_4$-mediated C–C bond formation, and explored the reaction mechanism using density functional theory (DFT).[3d] Other researchers have reported Ti alkoxyimido (Ti=N–OR) complexes and their reactivities towards internal alkynes;[4c] Ti hydrazides and their reactivities towards CO_2, CS_2, isocyanates, and organic nitriles;[5b,5c] and a dimeric Ti complex with terminal Ti=O with reactivity towards CO_2.[6a] Meanwhile, isonitriles could react with radicals, electrophiles, and nucleophiles with several advantages compared to the isoelectronic CO.[12–18] For example, the isonitrile reactions do not have to be performed under pressure, and the reactivities can be easily modulated by introducing substituents of different sizes and electron-donating/withdrawing properties onto the nitrogen.

Complex nitrogen-containing cyclic compounds are prevalent in natural products and pharmaceuticals.[19,20] For their synthesis, C–C bond formation reactions mediated by transition metals are the most important transformations.[21–25] Currently, the migratory insertion of isonitriles into metal–C bonds is a potentially important method for forming C–C bonds.[26–29] The resulting iminoacyl and metallaaziridine complexes are versatile intermediates in numerous transition metal-promoted stoichiometric and catalytic transformations. Xie *et al.* reported the migratory insertion of isonitriles into Ta–C bonds. They pointed out that alkyl and aryl isonitriles have different reactivity patterns, and the reaction products depend on the type and stoichiometry of the isonitriles.[27a,27b] Norton *et al.* described the migratory insertion of isonitriles into Zr–C bonds, and revealed the reversibility of the migratory insertion of *tert*-butyl (*t*Bu) isonitrile.[27d] In particular, the migratory insertion of isonitrile into titanacyclobutane complexes bearing two Cp* allows the stereocontrolled synthesis of valuable cyclobutanimines.[30] Recently, Norton *et al.* reported the reaction of Cp*(Cl)M(2,3-dimethylbutadiene) (M = Ti, **M1a**; M = Hf, **1a**) with isonitriles.[31] **M1a** can react with *N*-*t*Bu- and *N*-1-adamantyl (1-Ad)-substituted isonitriles at room temperature to form the bis-insertion product titanaaziridines. At elevated temperatures in benzene with pyridine, the titanaaziridine fragments to afford the complex cyclic compound of α-

[a]*School of Chemical Engineering, Anhui University of Science and Technology, Huainan 232001, People's Republic of China. E-mail: xbzhang_theochem@yahoo.com*

[b]*Department of Chemistry, Huaibei Normal University, Huaibei, Anhui 235000, People's Republic of China. E-mail: leiwang@chnu.edu.cn*

† Electronic supplementary information (ESI) available: Choice of calculated method, Schemes S1 and S2, Fig. S1–S12, Tables S1–S4, and calculated Cartesian coordinates and electronic energies (*E*) for the species involved in the work. See DOI: 10.1039/c7ra05680j

‡ These authors contributed equally to this paper.

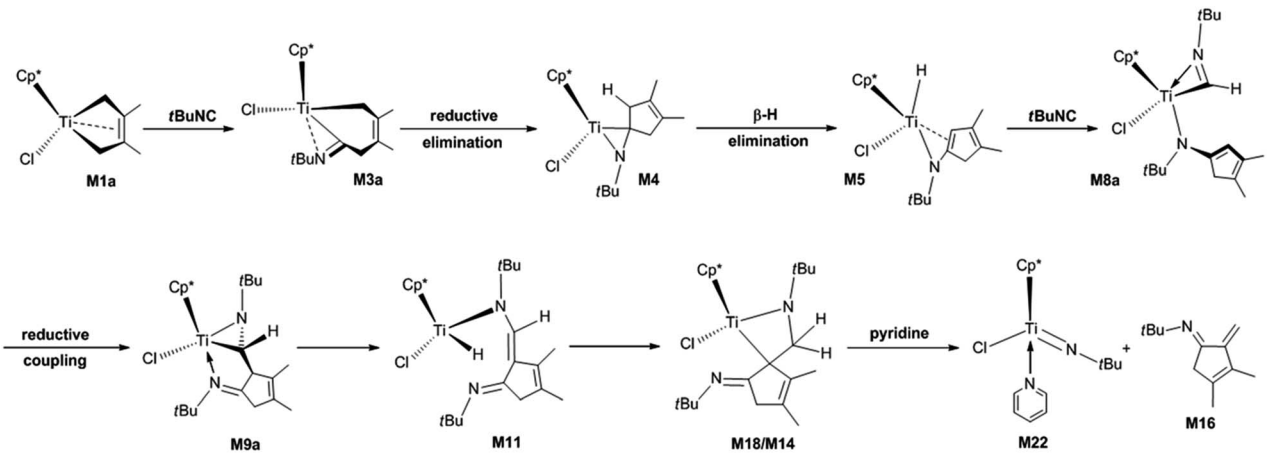

Scheme 1 Proposed mechanism for the formation of *N*-*t*Bu-substituted α-methylene cyclopentenimine *via* the four-membered titanacycle.

methylene cyclopent-3-enimine. The proposed mechanism for the reaction of **M1a** with *N*-*t*Bu-substituted isonitrile (*t*BuNC) is shown in Scheme 1. However, for the reaction of **1a** with *N*-2,6-dimethylphenyl (Ar)-substituted isonitrile (ArNC), diazahafnacyclopentane with the Ar groups is the final product, and the bis-insertion product of the isonitrile (the Hf analogue of titanaaziridine) is regarded as an intermediate instead. The work of Norton *et al.* not only expands the application of Ti complexes for C–C bond formation through the migratory insertion of isonitriles into Ti–C bond, but also provides a new method for synthesising complex cyclic compounds with potential bioactivity.

However, several important aspects about the reaction of **M1a** with isonitriles remain poorly understood: (1) the detailed mechanisms for the formation of titanaaziridines *via* bis-insertion and their fragmentations; (2) the effects of substituent groups on the nitrogen of isonitrile, in terms of the reaction mechanisms; (3) whether diazatitanacyclopentane, the Ti analogue of diazahafnacyclopentane, can be generated; and (4) if yes, which isonitriles should be used for this purpose. Herein, we used DFT calculations to theoretically examine the reactions of **M1a** with various isonitriles, in the hope of helping chemists explore new methods to form C–C bonds and synthesise new substances. Isonitriles bearing *t*Bu, methyl (Me), ethyl (Et), Ar, and 1-Ad groups were used as substrates to reveal their steric and electronic effects on the reaction mechanism and products. The substituent Et is more electron-donating than Me; *t*Bu, Ar and 1-Ad are bulkier than Me and Et; and *t*BuNC, ArNC, and 1-AdNC have been experimentally adopted by Norton *et al.*[31]

Computational details

All calculations were performed using the Gaussian 09 program package.[32] Molecular structures were optimised by the B3LYP/BS1 method.[32a,33,34] Solvent effects were taken into account by invoking the PCM solvation model using *n*-pentane and benzene,[35] which were experimentally used as solvents for crystallisation and reaction medium, respectively.[31] In the basis sets (BS1), the Ti and Cl atoms are described by the LANL2DZ basis sets improved with a set of f- or d-polarisation functions (α = 1.506 for Ti, α = 0.640 for Cl) with effective core potentials (ECPs),[36–40] while the other atoms are represented with the 6-311+G(d,p) basis sets, except for atoms on the *t*Bu, Me, Et, Ar, and 1-Ad substituent groups which are described by 6-31G basis sets.[41–43] As shown in ESI,† this theoretical model has been proven to be reliable, as it gives results in good agreement with experimental data. Meanwhile, frequency calculations were performed to confirm that the calculated species are minima (no imaginary frequency) or transition states (one and only one imaginary frequency), and to provide thermodynamic corrections at 1 atm and 298.15 K. Moreover, intrinsic reaction coordinate (IRC) calculations were carried out to ensure that the obtained transition states are correctly connected to the identified intermediates.[44] Finally, more accurate energies were calculated using the 6-311G(d,p) instead of the 6-31G basis sets in the BS1 (BS5). In order to take the dispersion effects into account, the B3LYP-D3/BS5//B3LYP/BS1 calculations on the optimum reaction pathways and important species were carried out at the same time.[32b,45] Natural bond orbital (NBO) analysis was performed at the stationary points, and the Wiberg bond indices (WBIs) and interaction energies between the Ti centre and other molecular moieties were computed by the NBO program as implemented in the G09 package.[32a] Corrected Gibbs free energies were used to describe the energetic profiles of the reactions.

Results and discussion

Mechanism of the reaction of M1a with *t*BuNC

We begin with the reaction of **M1a** with *t*BuNC, whose calculated reaction pathway is shown in Scheme 1. The coordination of the isonitrile to **M1a** and its subsequent migratory insertion into the Ti–C bond [Scheme S1(a)†] require an energy of 29.6 kcal mol^{-1}, which is too high for the reaction to occur. Instead, **M1a** is converted to **M1b** *via* **TSM1a–1b**, with the energy barrier of 16.6 kcal mol^{-1} and endergonic by 5.3 kcal mol^{-1} [Fig. 1(a)]. The dispersion-corrected energy barrier is 19.1 kcal mol^{-1}, which is larger than the uncorrected value. Therefore, the

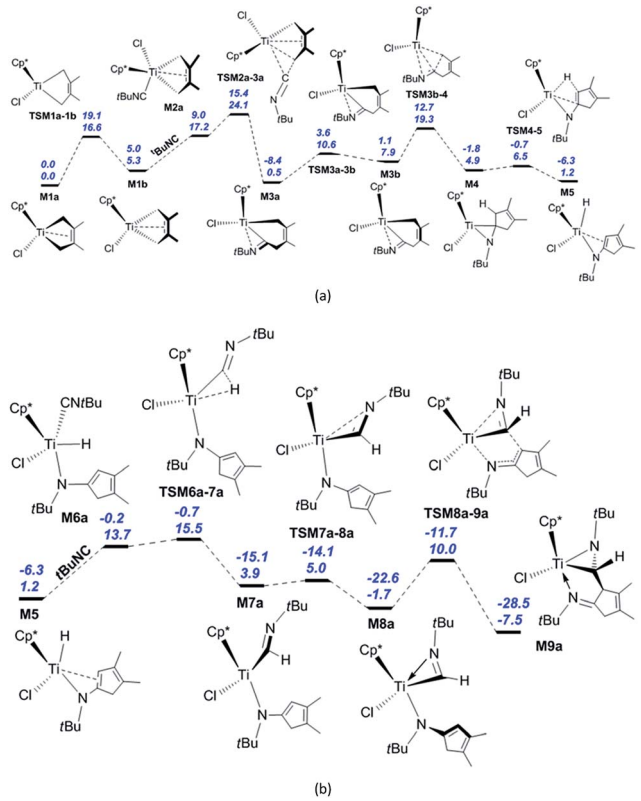

Fig. 1 (a) Energetic profiles for the isomerisation of **M1a** to **M1b**, migratory insertion of the first *t*BuNC into the Ti–C bond, C–C reductive elimination, β-H reductive elimination, and other elementary reaction steps. (b) Energetic profiles for the migratory insertion of the second *t*BuNC into Ti–H bond, C–C reductive coupling, and other elementary reaction steps. The Gibbs free energies are given in kcal mol^{-1} and the above values include the dispersion correction. Solvent: pentane.

dispersion effects increase the energy barrier of the isomerisation from **M1a** to **M1b**. **M1a** and **M1b** both feature the coordinated C^2–C^3 π-double bond, as evidenced by the lengths of Ti–C^2 and Ti–C^3 (2.35 and 2.35 Å in **M1a**, 2.38 and 2.38 Å in **M1b**, respectively; see Fig. S1†). The C^2=C^3 π-bond coordination to Ti is further confirmed by the WBIs of Ti–C^2 (0.29 for **M1a** and 0.28 for **M1b**) and Ti–C^3 (0.29 for **M1a** and 0.28 for **M1b**). The interaction energies between the C^2=C^3 π orbitals and the valence orbitals on Ti are calculated to be 52.2 kcal mol^{-1} for **M1a** and 54.4 kcal mol^{-1} for **M1b**, respectively. The isonitrile coordinates to **M1b** with the carbon atom end-on, a process that is endergonic by 11.9 kcal mol^{-1} due to the entropy reduction (−42.0 cal mol^{-1} K^{-1}). After the dispersion corrections, this endergonicity is reduced to 4.0 kcal mol^{-1}. Therefore, the dispersion effects significantly influence the isonitrile coordination. In **M2a**, the lengths of Ti–C^1 (2.27 Å) and Ti–C^4 (2.53 Å) are longer than that (2.15 Å) in **M1b**, and the structure of **M2a** is consistent with the coordinated C^2–C^3 π-bond (Ti–C^2 = 2.29 Å, Ti–C^3 = 2.41 Å). The calculated WBIs of Ti–C^2 and Ti–C^3 (0.42 and 0.24) confirm the C^2–C^3 π-bond coordination to the Ti centre in **M2a**. The subsequent migratory insertion of the isonitrile into the neighbouring Ti–C bond requires 6.9 kcal mol^{-1} to afford **M3a** with an exergonicity of 16.7 kcal mol^{-1}. The dispersion effects decrease the energy barrier of the isonitrile insertion into the Ti–C bond by 0.5 kcal mol^{-1} and increase the exergonicity by 0.7 kcal mol^{-1}. This energy requirement is much lower, and the endergonicity is larger compared to those of a similar insertion into the Pd^{III}–C bond reported by Yan *et al.* (15.4 and 7.7 kcal mol^{-1}, respectively).[26c] However, the reported activation energy for the Pd^{III} complex is much lower than that for the migratory insertion of isonitrile into Ti–C bond in **M2b** [23.4 kcal mol^{-1}; see Scheme S1(a)†]. Obviously, the energy required for isonitrile insertion into the metal–C bond varies greatly with the metal complex and the configuration. The energy barrier for the migratory insertion of isonitrile into the Ti=N bond reported by Clot and Mountford *et al.* is larger than our calculated value (14.0 *vs.* 6.9 kcal mol^{-1}).[5e] The reversibility of the migratory insertion of the isonitrile into Ti–C bond is consistent with that of *t*BuNC into the Zr–C bond.[27d] In **TSM2a–3a**, the C^5–C^4 σ-bond (1.92 Å) is formed, the Ti–C^4 distance (2.47 Å) is shortened, and C^5 changes from sp to sp^2 hybridisation, accompanied by the bending of the Ti–C^5–N^1 structure. In **M3a**, the N atom is coordinated to the Ti centre (Ti–N^1 = 2.06 Å), and the C^2–C^3 π-double bond is repelled from the Ti centre to create a 14-valence electron configuration. The calculated WBIs of Ti–C^2 and Ti–C^3 (0.03 and 0.05, respectively) are so small that the interaction between the Ti centre and the C^2–C^3 π-double bond can be ignored, and C^5–N^1 is a characteristic double bond (WBI = 1.72). The calculated interaction energy between the empty d orbital on the Ti centre and the lone pair on the nitrogen is about 97 kcal mol^{-1}, and the WBI of Ti–N^1 is 0.62. While the distorted five-membered titanacyle is converted to a six-membered one, ring tension is released so that the system is exergonic by 16.7 kcal mol^{-1}. Overcoming the energy barrier of 10.1 kcal mol^{-1}, **M3a** is converted to an isomer **M3b** (Ti–C^1 = 2.21 Å) *via* **TSM3a–3b**. The increased ring tension leads to the endergonicity of 7.4 kcal mol^{-1}. After considering the dispersion effects, the energy barrier of this isomerisation increases by 1.9 kcal mol^{-1} and the endergonicity increases by 2.1 kcal mol^{-1}. The reductive elimination from **M3b** produces the titanaaziridine **M4** (Ti–C^1 = 2.43 Å, C^5–C^1 = 1.50 Å) through **TSM3b–4** (Ti–C^1 = 2.36 Å, C^5–C^1 = 1.97 Å). This process involves breaking the Ti–C^1 bond and forming the C^5–C^1 bond, with the energy barrier and exergonicity of 11.4 and 3.0 kcal mol^{-1}, respectively. It is easily found that dispersion effects have a marginal influence on this process. In **M4** there is a strong agostic interaction between the Ti centre and C^1–H^1 bond, as evidenced by the lengths of Ti–H^1 (1.98 Å) and C^1–H^1 (1.17 Å). The calculated WBI of Ti and H^1 is 0.19, and the interaction energy between valence orbitals on Ti and C^1–H^1 σ orbitals is 70.9 kcal mol^{-1}. The subsequent β-H elimination *via* **TSM4–5** requires a relatively lower energy of 1.6 kcal mol^{-1} (Ti–C^5 = 2.26 Å, Ti–C^1 = 2.36 Å, Ti–H^1 = 1.72 Å, and C^1–H^1 = 1.51 Å) to furnish the Ti hydride **M5** (Ti–C^5 = 2.42 Å, Ti–C^1 = 2.62 Å) with an exergonicity of 3.7 kcal mol^{-1}. The small energy barrier and the exergonicity stem from the conjugation with another π-double bond. In **TSM4–5**, the Ti–C^5 and Ti–N^1 bonds are lengthened, the length of Ti–C^1 is shorter than that in **M4**, and

the C^5–C^1 single bond is changed to a π-double bond. In **M5**, the lengths of Ti–C^5 and Ti–C^1 indicate that there is a weak interaction between the Ti centre and the C^5–C^1 π-double bond. The coordination of a second isonitrile to **M5** generates **M6a** (Ti–C^7 = 2.14 Å, Ti–H^1 = 1.68 Å) with an endergonicity of 12.5 kcal mol^{-1} [Fig. 1(b)]. After the dispersion corrections, the endergonicity is decreased to 6.1 kcal mol^{-1}. In **M6a**, the C^5–C^1 π-double bond is repelled from the Ti centre to maintain a 14-valence electron configuration. Then, the migratory insertion of the isonitrile into the Ti–H bond generates **M7a** *via* **TSM6a–7a** (Ti–C^7 = 2.06 Å, Ti–H^1 = 1.71 Å, and C^7–H^1 = 1.66 Å) with an energy barrier of only 1.8 kcal mol^{-1}, and the system is exergonic by 9.8 kcal mol^{-1}. The dispersion effects increase the exergonicity of the system by 5.1 kcal mol^{-1}. Compared to **M6a**, the bond parameters of **TSM6a–7a** imply that it is an early transition state. Through the N coordination, **M7a** is easily converted to the 14-valence electron complex **M8a** *via* **TSM7a–8a**, overcoming a negligible energy barrier of 1.1 kcal mol^{-1}. The exergonicity (5.6 kcal mol^{-1}) originates from the higher stability of **M8a** compared to **M7a**. The dispersion corrections lead to an increase of the exergonicity by 1.9 kcal mol^{-1}. Subsequently, **M8a** undergoes the C–C reductive coupling to afford the titanaaziridine **M9a** *via* **TSM8a–9a** (Ti–N^1 = 2.15 Å, and C^7–C^1 = 2.10 Å), a process that requires 11.7 kcal mol^{-1} and releases 5.8 kcal mol^{-1} in energy. The dispersion-corrected energy barrier is 10.9 kcal mol^{-1}, which is 0.8 kcal mol^{-1} less than the uncorrected value.

Among the elementary reaction steps, the coordination of the isonitrile, migratory insertion of the isonitrile into Ti–C bond, isomerisation of the six-membered titanacycle, C–C reductive elimination, and C–C reductive coupling require relatively higher energies. With the formation of **M9a**, the reaction is exergonic by 7.5 kcal mol^{-1}. Three steps, namely the isomerisation of **M1a** to **M1b**, the coordination of the first isonitrile, and its subsequent migratory insertion into the Ti–C bond determine the apparent activation energy of the whole reaction, which is 24.1 kcal mol^{-1}. Considering the dispersion effects, the exergonicity for the formation of **M9a** is increased to 28.5 kcal mol^{-1}. Owing to the much reduced endergonicity for the isonitrile coordination, the isomerisation of **M1a** to **M1b** becomes the sole elementary reaction for determining the reaction rate. This feature is consistent with the fact that no intermediates (**M3a**, **M4**, **M5** or **M8a**) have been found experimentally.[31] The coordination of the second isonitrile to **M3a** and its subsequent migratory insertion to generate bis(iminoacyl) titanacycle **M7b** require the energy of 39.1 kcal mol^{-1} [Scheme S1(b)†], which is too high under typical experimental conditions. Indeed, products related to the titanacycle **M7b** were not found experimentally, although two relevant enantiomers including **M9a** were experimentally isolated as green powders.[31] The calculated activation energy for the migratory insertion of the isonitrile into the Ti–C bond in **M6b** (16.6 kcal mol^{-1}) is comparable to the reported value for the Pd^{III} system.[26c]

Next, the fragmentation of **M9a** into the Ti imido complex **M15** and *N*-*t*Bu-substituted α-methylene cyclopentenimine **M16** is studied. Initially, the dissociation of Ti–N(ketimine) bond in **M9a** affords **M10** (Fig. 2) with the endergonicity of 6.7 kcal mol^{-1}, whereas N(ketimine) denotes the nitrogen atom in the ketimine. After the dispersion corrections, the endergonicity is increased to 11.6 kcal mol^{-1}. Then, the β-H elimination produces the Ti hydride complex **M11** (Ti–N^1 = 3.56 Å, Ti–N^2 = 1.93 Å, and Ti–H^2 = 1.67 Å) with a 12-valence electron configuration *via* **TSM10–11** (Ti–H^2 = 1.75 Å, C^1–H^2 = 1.49 Å). This process requires 14.5 kcal mol^{-1} and is endergonic by 6.4 kcal mol^{-1}. The dispersion-corrected energy barrier and endergonicity both decrease by about 1 kcal mol^{-1} relative to the

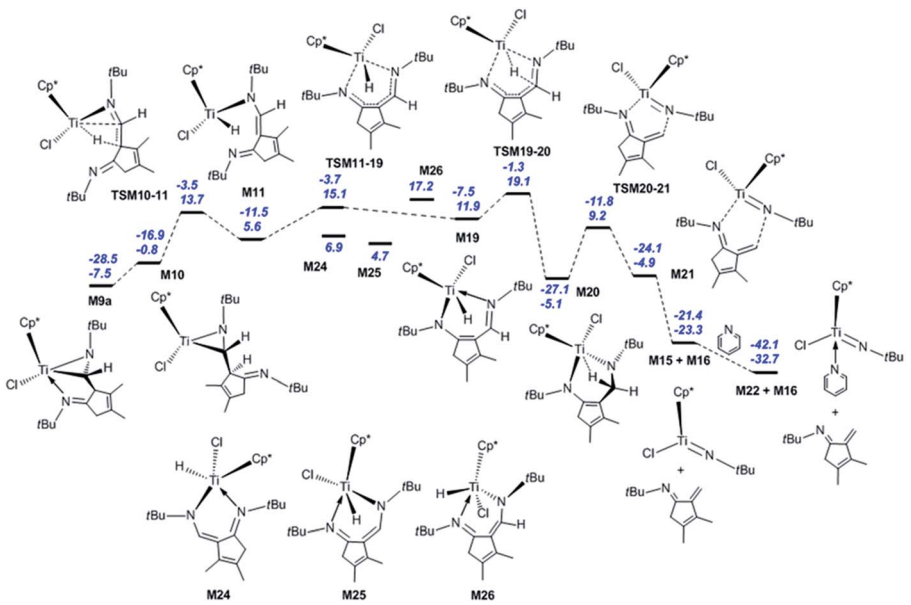

Fig. 2 Energetic profiles for the fragmentation of the titanaaziridine **M9a** *via* the β-H elimination reaction pathway. The Gibbs free energies are given in kcal mol^{-1} and the above values include the dispersion correction. Solvent: pentane.

uncorrected values. In **TSM10–11**, the C^1–H^2 bond is almost broken and the Ti–H^2 bond is almost formed. In the product **M11**, the length of Ti–N^1 indicates that there is no interaction between the Ti centre and the N(ketimine) atom. In the work by Norton *et al.*, a four-membered titanacycle (**M14** or **M18**) is supposed to be an intermediate in the fragmentation reaction of **M9a**.[31] Indeed, **M14** is the relatively stable species in this study (with an energy of −1.6 kcal mol^{-1} referred to **M1a** and 2 molecules of *t*BuNC), and it easily fragments to form the target products with an energy barrier of 8.7 kcal mol^{-1} [Fig. S2(a)†]. The reaction pathway to the four-membered titanacycle **M14** *via* a zwitterionic intermediate **M13** (generated by the addition of Ti–H across the double bond in **M11**) requires a high energy (at least 35.4 kcal mol^{-1}), due to the charge separation in **M13**. Another reaction pathway to form **M18** through an intermediate **M17** (produced by the hydrogen transfer to Cp* in the metal hydride **M11**) needs to overcome an energy barrier of at least 40.1 kcal mol^{-1}. The apparent energy barriers of these two routes are too high, thus the corresponding reactions cannot proceed under experimental conditions. Thus, our attempts to find a feasible fragmentation pathway for **M11** *via* four-membered titanacycle intermediate failed. The proposed fragmentation mechanism for **M9a** is shown in Scheme 2(a). Along the β-H elimination reaction pathway, **M11** isomerises into **M19** (Ti–N^1 = 2.13 Å, Ti–N^2 = 2.15 Å, Ti–H^2 = 1.63 Å, and C^7–N^2 = 1.32 Å) *via* **TSM11–19** (Ti–N^1 = 2.40 Å, Ti–N^2 = 1.97 Å), overcoming an energy barrier of 9.5 kcal mol^{-1} and with an endergonicity of 6.3 kcal mol^{-1} (Fig. 2). Considering the dispersion effects, the energy barrier and endergonicity decrease by 1.7 and 2.3 kcal mol^{-1}, respectively. In this process, the N^1 atom, *i.e.*, N(ketimine), gradually approaches the Ti centre. In **M19**, the Ti–N^2 bond is slightly longer than the Ti–N^1 bond, and the structure of six-membered titanacycle is stabilised by electron delocalisation. Then, **M19** undergoes the addition of Ti–H across the azaallyl double bond, and is thus converted to **M20** (Ti–N^2 = 1.86 Å, Ti–H^2 = 2.17 Å, and C^7–N^2 = 1.49 Å) *via* **TSM19–20** (Ti–N^2 = 1.89 Å, Ti–H^2 = 1.70 Å, C^7–H^2 = 1.89 Å, and C^7–N^2 = 1.41 Å), with an energy barrier of 7.2 kcal mol^{-1} and the exergonicity of 17.0 kcal mol^{-1}. The dispersion-corrected energy barrier is reduced to 6.2 kcal mol^{-1}, and the exergonicity is increased to 19.6 kcal mol^{-1}. In **TSM19–20**, the C^7–H^2 distance is much longer than that of the usual C–H bond, and the Ti–H^2 and C^7–N^2 bonds in **TSM19–20** are slightly longer than those in **M19**. In **M20**, the length of Ti–H^2 implies the existence of a strong agostic interaction between the Ti centre and the C^7–H^2 σ bond, and the interaction energy is calculated to be 42.3 kcal mol^{-1}. **M20** is lower in energy than the four-membered titanacycles **M14** and **M18**. Therefore, the conversion of **M11** to **M20** *via* **M19** is kinetically and thermodynamically more favourable, with an energy barrier of 13.5 kcal mol^{-1} and the exergonicity of 10.7 kcal mol^{-1}. **M20** fragments to **M15** and **M16** *via* **TSM20–21** (Ti–N^1 = 2.26 Å, C^7–N^2 = 2.07 Å, and Ti–H^2 = 2.18 Å). In this step, the system overcomes an energy barrier of 14.3 kcal mol^{-1} and releases 18.2 kcal mol^{-1} in energy. The large exergonicity is mainly ascribed to increased entropy (65.2 cal mol^{-1} K^{-1}). Our calculated results are similar to the reported energy barrier (11.3 kcal mol^{-1}) and exergonicity (17.7 kcal mol^{-1}) for the fragmentation of the titanacycle produced through the cycloaddition reaction of Ti alkoxyimido complex and ketone.[46] In sharp contrast to the large exergonicity, after the dispersion corrections this fragmentation step becomes endergonic by 5.7 kcal mol^{-1}, and the energy

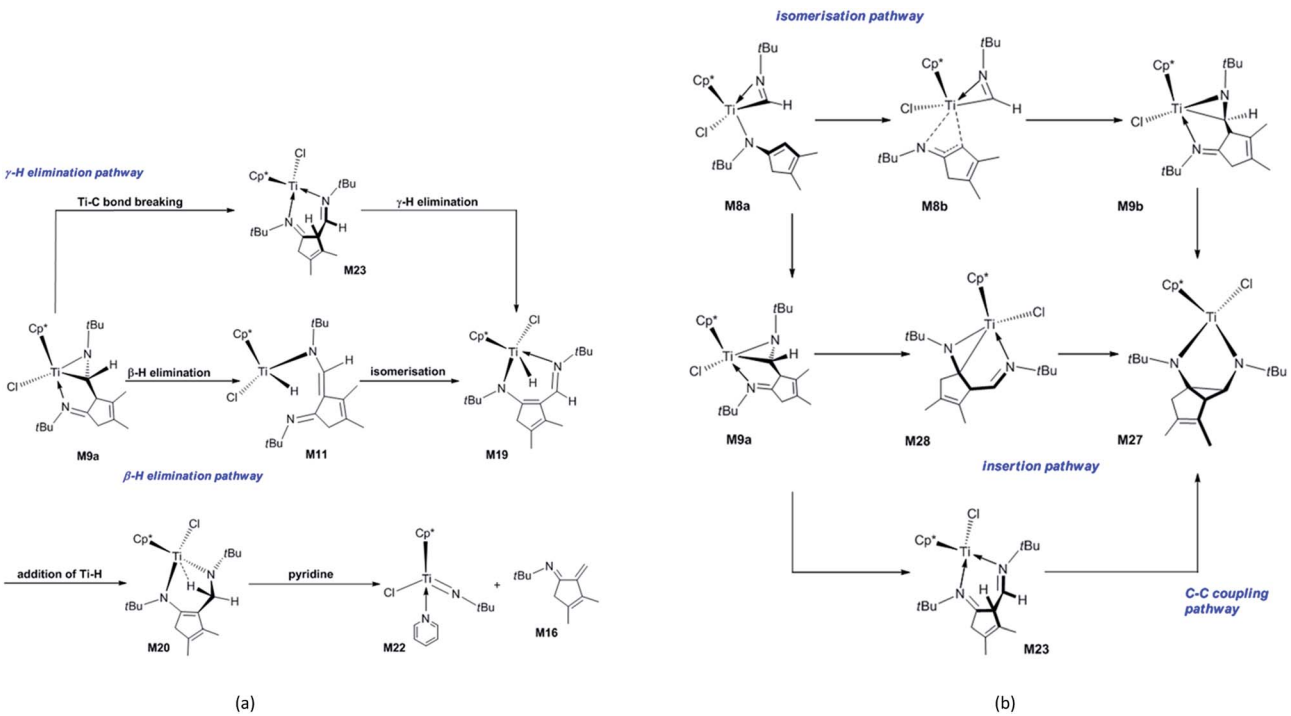

Scheme 2 Proposed mechanisms for (a) the fragmentation of the titanaaziridine **M9a** and (b) forming diazatitanacyclopentane **M27**.

barrier increases by 1.0 kcal mol^{-1}. The structure of **TSM20–21** is stabilised by a strong agostic interaction between the Ti centre and the C^7–H^2 σ bond. The formed **M15** is trapped by a pyridine to generate **M22**, with an exergonicity of 9.4 kcal mol^{-1}. Considering the dispersion corrections, the exergonicity is increased to 20.7 kcal mol^{-1}. In this reaction mechanism, the β-H elimination and fragmentation of six-membered titanacycle have higher energy barriers; and the addition of Ti–H and the trapping of the Ti imido complex by pyridine release more energies. This reaction pathway requires the apparent activation energy of 27.2 kcal mol^{-1} (after the dispersion corrections), thus it is kinetically feasible under the experimental conditions, and the large exergonicity of 13.6 kcal mol^{-1} (after the dispersion corrections) makes the fragmentation thermodynamically favourable and irreversible. Because the reaction was experimentally carried out in benzene, we re-calculated the overall energetic profile of the reaction using benzene as solvent. The results are almost the same as that in *n*-pentane (Table S1†), because both *n*-pentane and benzene are nonpolar solvents. In the γ-H elimination reaction pathway, **M9a** is converted to **M23** with the Ti–C bond breaking *via* **TSM9a–23**, overcoming an energy barrier of 24.7 kcal mol^{-1} [Fig. S2(b)†], and the process is endergonic by 21.3 kcal mol^{-1}. Then, **M23** undergoes γ-H elimination and is converted to **M19** *via* **TSM23–19**, and this step has an energy barrier of 13.6 kcal mol^{-1} and is exergonic by 1.9 kcal mol^{-1}. The required apparent activation energy for this fragmentation pathway (34.9 kcal mol^{-1}) is larger than that of the β-H elimination reaction pathway discussed above (26.7 kcal mol^{-1} without dispersion correction), thus the γ-H elimination reaction pathway is kinetically unfavourable for the titanaaziridine with the *t*Bu groups. The direct conversion of **M11** to **M20** through the addition of Ti–H across the C=C double bond requires an energy of 19.3 kcal mol^{-1}, which is larger than 13.3 kcal mol^{-1} for the conversion from **M11** to **M20** *via* **M19** (Fig. 2), thus this possibility is also ruled out. In addition, three stationary points (**M24**, **M25**, and **M26**) were localised; however, none of them is located on the optimum reaction pathway.

In order to explore the possible formation of the diazatitanacyclopentane **M27**, three reaction mechanisms are considered [Scheme 2(b)]. (1) In the insertion reaction pathway, the intermediate **M28** is 17.3 kcal mol^{-1} higher in energy than **M9a** [Fig. 3(a)]. **M28** undergoes the insertion of C=N into the Ti–C bond *via* **TSM28–27** to generate **M27**, with an energy barrier of 20.6 kcal mol^{-1} and exergonic by 0.8 kcal mol^{-1}. (2) In the C–C coupling reaction pathway, through the C–C coupling, **M23** is converted to **M27**, overcoming an energy of 11.2 kcal mol^{-1} and exergonic by 4.8 kcal mol^{-1}. (3) In the isomerisation reaction pathway, **M8a** firstly isomerises into **M8b** *via* **TSM8a–8b**, with an energy barrier of 19.6 kcal mol^{-1} and endergonic by 14.9 kcal mol^{-1} [Fig. 3(b)]. Then, **M8b** undergoes C–C reductive coupling to give **M9b** (an isomer of **M9a**) *via* **TSM8b–9b**. This step requires an energy of 8.0 kcal mol^{-1}, and is exergonic by 9.4 kcal mol^{-1}. Through the insertion of C=N into the Ti–C bond, **M9b** is converted to the target compound **M27** *via* **TSM9b–27**, with an energy barrier of 25.2 kcal mol^{-1} and the endergonicity of 5.1 kcal mol^{-1}. In contrast, the C–C coupling reaction pathway is more favourable, but it still requires a high apparent activation energy of 32.5 kcal mol^{-1}, with an endergonicity of 16.5 kcal mol^{-1} referred to **M9a**. The analyses above show that for *t*BuNC, the formation of diazatitanacyclopentane **M27** is kinetically and thermodynamically unfavourable.

Effects of substituent groups on reaction mechanisms and products

In order to reveal the steric and electronic effects of isonitrile *N*-substituent groups on the mechanisms and products, the energetic profiles of the reactions using MeNC, EtNC, ArNC, and 1-AdNC instead of *t*BuNC were calculated (Fig. S3–S10†). The reaction pathways are shown in Scheme 3, and the results are summarised in Tables 1 and 2.

For the bis-insertion reaction of MeNC, we found the following results from Table 1. (1) The isonitrile coordinates to **M1b** and Ti hydride **6^{Me}** [Scheme 3(a)], endergonic by 11.7 and 6.4 kcal mol^{-1}, respectively. The endergonicity is less than that

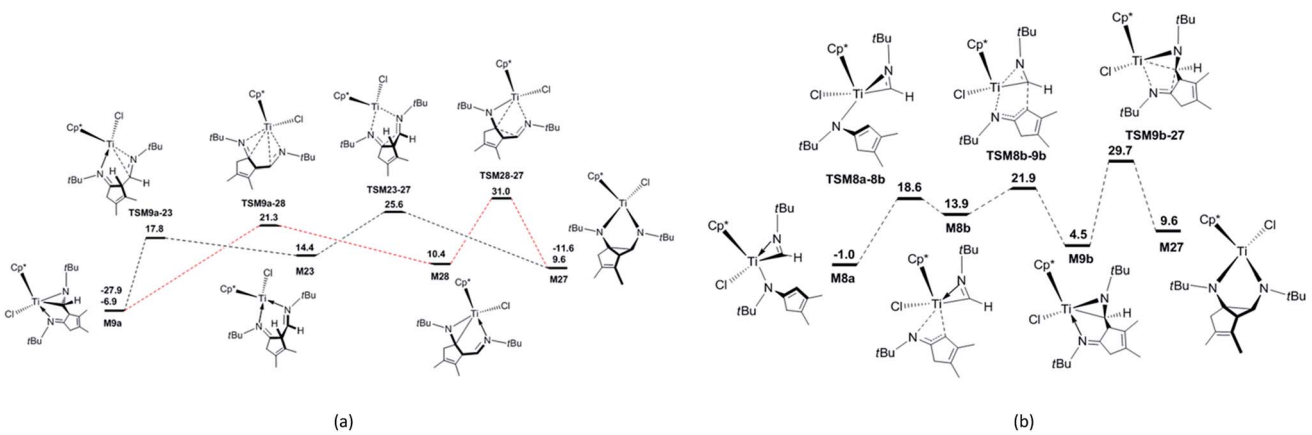

Fig. 3 Energetic profiles for the formation of the diazatitanacyclopentane **M27** (a) *via* the insertion and the C–C coupling reaction pathways, and (b) *via* the isomerisation reaction pathway. The Gibbs free energies are given in kcal mol^{-1} and the above values include the dispersion correction. Solvent: benzene.

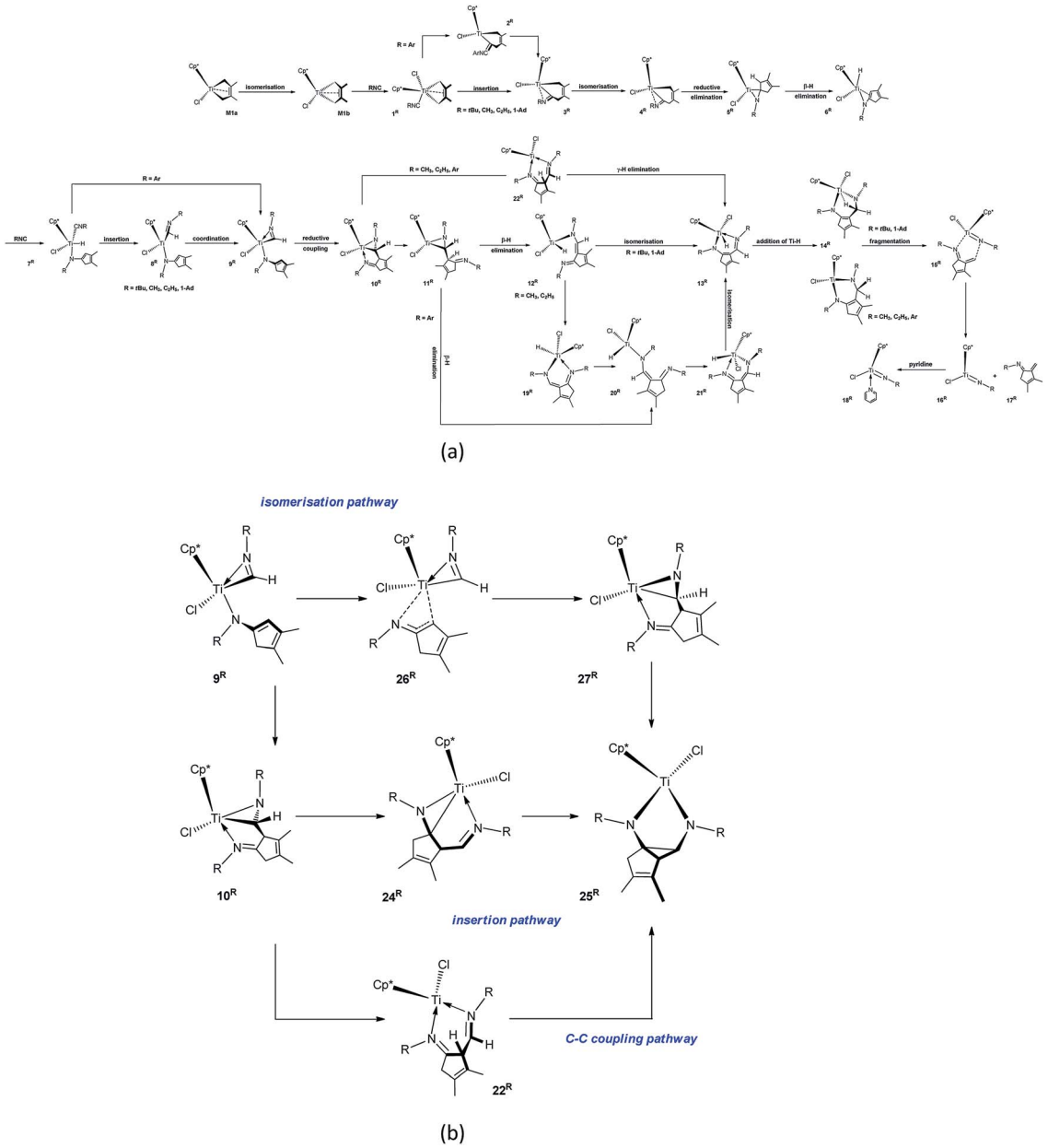

Scheme 3 The calculated pathways for (a) forming cyclic α-methylene cyclopentenimine through the reaction of **M1a** with *N*-R-substituted isonitriles and (b) forming diazatitanacyclopentane 25^{R} (R = *t*Bu, Me, Et, Ar, and 1-Ad).

in the case of *t*BuNC. Although the Me group is less electron-donating than the *t*Bu group, the smaller size of the former leads to less repulsion between the substituents relative to the latter. The reduced repulsion causes less energy increase for the MeNC-coordinated complexes ($\mathbf{1}^{\mathbf{Me}}$ and $\mathbf{7}^{\mathbf{Me}}$). The entropy change caused by the coordination of *t*BuNC to **M8a** is only 6.6 cal mol^{-1} K^{-1} larger than that caused by the coordination of MeNC to $\mathbf{6}^{\mathbf{Me}}$ (−36.5 cal mol^{-1} K^{-1} for *t*BuNC and −29.9 cal mol^{-1} K^{-1} for MeNC). (2) The isonitrile migratory insertion into the Ti–C bond, the isomerisation of Ti complex, C–C reductive elimination, β-H elimination, and C–C reductive coupling require less energies for MeNC than for *t*BuNC (4.3 *vs.* 7.3, 7.0 *vs.* 9.8, 9.3 *vs.* 11.5, 1.2 *vs.* 1.6, and 10.9 *vs.* 11.7 kcal mol^{-1}, respectively). The bulkier groups make the structures of transition states more congested than that of the reactants, thus the activation energies of elementary reactions are larger for *t*BuNC than for MeNC. The MeNC migratory insertion into the Ti–H bond needs to overcome almost the same energy barrier as that for *t*BuNC (1.9 *vs.* 1.8 kcal mol^{-1}). These elementary reactions are either much more exergonic or endergonic relative to that for *t*BuNC, except for the isonitrile insertion into the Ti–H bond that has a smaller exergonicity (7.5 *vs.* 9.6 kcal mol^{-1}). The N coordination in $\mathbf{8}^{\mathbf{Me}}$ is very exergonic (10.6 kcal mol^{-1}). These differences are mainly attributed to the distinct steric effects of the Me and *t*Bu groups on the intermediates. (3) Without considering the dispersion corrections, the overall bis-insertion

Table 1 The calculated Gibbs free energies (ΔG; in kcal mol^{-1}) for species in the reaction pathways of bis-insertion and fragmentation of bis-insertion product in the case of *t*BuNC, MeNC, EtNC, ArNC, and 1-AdNC [referred to **M1a** and RNC (or 2RNC)][a]

	ΔG				
Mol.	*t*Bu	Me	Et	Ar	1-Ad
$\mathbf{1^R}$	17.1	16.7	16.7	17.6	17.0
$\mathbf{TS1^R}$–$\mathbf{3^R}$ (for R = Ar, $\mathbf{TS1^R}$–$\mathbf{2^R}$)	24.4	21.0	20.9	21.7	24.6
$\mathbf{2^R}$				12.4	
$\mathbf{TS2^R}$–$\mathbf{3^R}$				12.9	
$\mathbf{3^R}$	1.0	−3.1	−2.3	5.0	1.5
$\mathbf{TS3^R}$–$\mathbf{4^R}$	10.8	3.9		8.9	
$\mathbf{4^R}$	8.0	0.9	2.3	6.4	9.0
$\mathbf{TS4^R}$–$\mathbf{5^R}$	19.5	10.2	11.3	14.7	19.9
$\mathbf{5^R}$	5.2	−4.9	−3.5	−1.5	5.4
$\mathbf{TS5^R}$–$\mathbf{6^R}$	6.8	−3.7		0.3	
$\mathbf{6^R}$	1.4	−10.1		−4.1	
$\mathbf{7^R}$	14.1	−3.7		8.0	
$\mathbf{TS7^R}$–$\mathbf{8^R}$ (for R=Ar, $\mathbf{TS7^R}$–$\mathbf{9^R}$)	15.9	−1.8		8.1	
$\mathbf{8^R}$	4.5	−11.2			
$\mathbf{TS8^R}$–$\mathbf{9^R}$	5.5	−8.1			
$\mathbf{9^R}$	−1.0	−21.8	−17.5	0.1	−1.0
$\mathbf{TS9^R}$–$\mathbf{10^R}$	10.7	−10.9		12.8	
$\mathbf{10^R}$	−6.9	−31.0	−25.2	−6.1	−5.7
$\mathbf{11^R}$	−0.1	−15.4	−12.2	−5.0	3.0
$\mathbf{TS11^R}$–$\mathbf{12^R}$ (for R = Ar, $\mathbf{TS11^R}$–$\mathbf{20^R}$)	14.5	1.3	3.8	11.3	15.2
$\mathbf{12^R}$	6.5	−9.1	−6.2		7.1
$\mathbf{TS12^R}$–$\mathbf{13^R}$ (for R = Me, Et, $\mathbf{TS12^R}$–$\mathbf{19^R}$)	15.7	−9.9			17.8
$\mathbf{13^R}$	12.6	−22.8	−17.2	4.9	15.0
$\mathbf{TS13^R}$–$\mathbf{14^R}$	19.8	−10.1	−4.3	16.4	21.8
$\mathbf{14^R}$	−4.8	−40.6	−36.7	−13.7	−2.5
$\mathbf{TS14^R}$–$\mathbf{15^R}$	9.9	−19.7		0.3	
$\mathbf{15^R}$	−4.1	−34.2		−10.3	
$\mathbf{16^R}$ + $\mathbf{17^R}$	−23.6	−33.2		−35.8	
$\mathbf{18^R}$ + $\mathbf{17^R}$	−32.2	−42.2	−40.9	−43.0	−31.5
$\mathbf{19^R}$	7.6	−31.7	−25.4		
$\mathbf{20^R}$		−12.1	−9.9	−2.9	
$\mathbf{21^R}$	18.0	−20.4	−16.7	−7.3	
$\mathbf{TS21^R}$–$\mathbf{13^R}$		−20.7	−13.7	5.8	
$\mathbf{TS10^R}$–$\mathbf{22^R}$	17.8	−10.5	−4.7		
$\mathbf{22^R}$	14.4	−14.3	−11.9	16.9	
$\mathbf{TS22^R}$–$\mathbf{13^R}$ (for R = Et, Ar, $\mathbf{TS22^R}$–$\mathbf{23^R}$)	28.0	0.1	4.4	26.4	
$\mathbf{23^R}$			−16.4	0.6	
$\mathbf{TS23^R}$–$\mathbf{14^R}$				16.7	

[a] (1) **TSA–B** denotes a transition state connected species **A** and **B**; (2) $\mathbf{23^R}$ is an isomer of $\mathbf{13^R}$; (3) solvent: benzene.

reaction of MeNC requires 21.0 kcal mol^{-1}, which is smaller than that of *t*BuNC, and releases more energy (31.0 kcal mol^{-1}). In the β-H elimination reaction pathway, the energy required for dissociating the Ti–N(ketimine) bond in $\mathbf{10^{Me}}$ is much larger than that in $\mathbf{10^{tBu}}$ (15.6 *vs.* 6.8 kcal mol^{-1}). Overcoming an energy barrier of 16.7 kcal mol^{-1}, $\mathbf{11^{Me}}$ undergoes the β-H elimination to afford the Ti hydride $\mathbf{12^{Me}}$ *via* $\mathbf{TS11^{Me}}$–$\mathbf{12^{Me}}$ with an endergonicity of 6.3 kcal mol^{-1}. In $\mathbf{TS11^{Me}}$–$\mathbf{12^{Me}}$, the length of Ti–H^2 (1.76 Å; Fig. S11†) is marginally longer than that in **TSM10–11** (1.75 Å), and that of C^1–H^2 (1.47 Å) is shorter than that in **TSM10–11** (1.50 Å). $\mathbf{12^{Me}}$ is easily converted to the six-membered titanacycle $\mathbf{19^{Me}}$ through the rotation of the Cp*TiClH segment about the Ti–N^2 σ-bond, and the re-coordination of the N(ketimine) atom to the Ti centre. The energy barrier in this step is negligible, and the system is highly exergonic (22.6 kcal mol^{-1}) mainly due to the coordination of the N(ketimine). The electron delocalisation stabilises the nearly planar six-membered structure of $\mathbf{19^{Me}}$. The dissociation of the Ti–N(ketimine) bond in $\mathbf{19^{Me}}$ generates $\mathbf{20^{Me}}$ with an endergonicity of 19.6 kcal mol^{-1}. Through the rotation of Cp*TiClH segment about the N^2–C^7 bond and re-coordination of the N(ketimine) atom to the Ti centre, $\mathbf{20^{Me}}$ is converted to $\mathbf{21^{Me}}$ with an exergonicity of 8.3 kcal mol^{-1}. $\mathbf{21^{Me}}$ rapidly isomerises to $\mathbf{13^{Me}}$, slightly exergonic by 2.4 kcal mol^{-1}. Subsequent addition of Ti–H requires an energy of 12.7 kcal mol^{-1} and is exergonic by 17.8 kcal mol^{-1}, both values are larger than those in the case of *t*BuNC. Unlike **M20**, there is no agostic interaction between the Ti centre and the C^7–H^2 bond in $\mathbf{14^{Me}}$, since the weaker repulsion between the Cp* and Me groups on nitrogen makes the six-membered titanacycle more planar. The lengths of Ti–H^2 and C^7–H^2 indicate that $\mathbf{TS13^{Me}}$–$\mathbf{14^{Me}}$ is an early transition state. Overcoming an energy barrier of 20.9 kcal

Table 2 The calculated Gibbs free energies (ΔG; in kcal mol^{-1}) for species in the reaction pathways of forming diazatitanacyclopentane $\mathbf{25^R}$ in the case of *t*BuNC, MeNC, EtNC, ArNC, and 1-AdNC [referred to **M1a** and RNC (or 2RNC)][a]

	ΔG				
Mol.	*t*Bu	Me	Et	Ar	1-Ad
$\mathbf{10^R}$	−6.9	−31.0	−25.2	−6.1	−5.7
$\mathbf{TS10^R–24^R}$	21.3	−9.8	−1.8	18.9	23.1
$\mathbf{24^R}$	10.4	−22.1	−16.4	−5.4	10.9
$\mathbf{TS24^R–25^R}$	31.0	−9.6	−6.0	9.4	32.6
$\mathbf{25^R}$	8.9	−28.2	−23.2	−13.7	11.1
$\mathbf{TS10^R–22^R}$	17.8	−10.5	−4.7		19.4
$\mathbf{22^R}$	14.4	−14.3	−11.9	16.9	19.2
$\mathbf{TS22^R–25^R}$	25.6	−6.8	−2.3	21.9	28.1
$\mathbf{9^R}$	−1.0	−21.8	−17.5	0.1	−1.0
$\mathbf{TS9^R–26^R}$ (R = Ar, $\mathbf{TS9^R–26IS^R}$)	18.6	−11.6	−6.5	3.1	20.0
$\mathbf{26IS^R}$				1.6	
$\mathbf{TS26IS^R–26^R}$				14.5	
$\mathbf{26^R}$	13.9	−12.8	−7.7	7.0	15.5
$\mathbf{TS26^R–27^R}$	21.9	−5.7	−0.9	15.6	23.5
$\mathbf{27^R}$	4.5	−23.7	−19.4	−9.1	5.8
$\mathbf{TS27^R–25^R}$	29.7	−13.4	−8.7	3.9	30.9

[a] (1) **TSA–B** denotes a transition state connected species **A** and **B**; (2) 26ISR is an isomer of $\mathbf{26^R}$; (3) solvent: benzene.

mol^{-1}, $\mathbf{14^{Me}}$ fragments to form the Ti imido complex $\mathbf{16^{Me}}$ and *N*-Me-substituted α-methylene cyclopentenimine $\mathbf{17^{Me}}$, with the endergonicity of 7.4 kcal mol^{-1}. This endergonicity is in sharp contrast to the large exergonicity for **M20**, which is ascribed to increased electronic energy due to the formation of the intermediate $\mathbf{15^{Me}}$ featuring the coordinated N(ketimine) atom. The lengths of Ti–N^1 and C^7–N^2 in $\mathbf{15^{Me}}$ are shorter than those in **M21** (2.24 *vs.* 2.58 Å and 3.18 *vs.* 3.32 Å, respectively), indicating that the increase of entropy during the fragmentation of $\mathbf{14^{Me}}$ is less than that in the case of **M20** (5.3 *vs.* 10.5 cal mol^{-1} K^{-1}). In the absence of pyridine, the final reaction product with MeNC is possibly the titanacycle $\mathbf{14^{Me}}$. Clearly, the dissociation of the Ti–N(ketimine) bond and the subsequent β-H elimination determine the apparent activation energy barrier of the reaction. After the dispersion corrections, this β-H elimination reaction pathway to $\mathbf{14^M}$ requires the energy of 32.6 kcal mol^{-1} and is exergonic by 10.5 kcal mol^{-1} with reference to $\mathbf{10^{Me}}$ (Fig. S4†). In the γ-H elimination reaction pathway, compared to that for *t*BuNC, the breaking of Ti–C bond requires less energy and is less endergonic (20.5 *vs.* 16.7 kcal mol^{-1}) for MeNC. The length of Ti–C bond in $\mathbf{10^{Me}}$ is longer than that in **M9a** (2.120 *vs.* 2.095 Å), indicating that the Ti–C bond in $\mathbf{10^{Me}}$ is stronger than that in **M9a**. Also, the γ-H elimination requires slightly more energy (14.4 kcal mol^{-1}) and releases a large amount of energy (8.5 kcal mol^{-1}). Considering the dispersion effects, the overall γ-H elimination reaction pathway needs to overcome an energy of 32.3 kcal mol^{-1} (Fig. S4†). Given the small difference in the apparent activation energies (0.3 kcal mol^{-1}) and the calculation errors, these two fragmentation pathways for $\mathbf{10^{Me}}$ compete with each other. Compared to the case of **M9a**, the fragmentation of $\mathbf{10^{Me}}$ needs to overcome a higher energy barrier and releases less energy. For the formation of the diazatitanacyclopentane $\mathbf{25^{Me}}$, among three suggested reaction pathways [Scheme 3(b)], the insertion reaction pathway is kinetically most favourable (Table 2). However, this reaction is thermodynamically unfavourable compared to the formation of *N*-Me-substituted α-methylene cyclopentenimine.

Conclusions for the substrate EtNC are the same as those for MeNC. When the Me group is replaced by Et, the required energy for the migratory insertion of the first isonitrile (EtNC) into Ti–C is slightly reduced (4.2 *vs.* 4.3 kcal mol^{-1}; Table 1), but the system is less exergonic (19.0 *vs.* 19.8 kcal mol^{-1}). It is well known that the Et group is larger in size but also more electron-donating than the Me group. Their combined effect is a slight reduction of the activation energy for EtNC insertion into Ti–C bond compared to MeNC insertion. The C–C reductive elimination from $\mathbf{4^{Et}}$ affords $\mathbf{5^{Et}}$, overcoming an energy barrier of 9.0 kcal mol^{-1} and exergonic by 5.8 kcal mol^{-1}. The more electron-donating Et group leads to a reduction of 0.3 kcal mol^{-1} for the energy barrier of C–C reductive elimination compared to MeNC. It can be inferred that, without considering the dispersion corrections, the formation of the titanaaziridine $\mathbf{10^{Et}}$ requires an energy of 20.9 kcal mol^{-1} and exergonic by 25.2 kcal mol^{-1}. Compared to the fragmentation of $\mathbf{10^{Me}}$, (1) the dissociation of the Ti–N(ketimine) bond and β-H elimination in the β-H elimination reaction pathway, and the dissociation of Ti–C bond in the γ-H elimination reaction pathway are both less endergonic; (2) the coordination of the N(ketimine) atom in the β-H elimination reaction pathway and the γ-H elimination are less exergonic; and (3) the required energy for β-H elimination decreases by 0.7 kcal mol^{-1}. In the transition state for β-H elimination, there is the formation of an azaallyl structure. A more electron-donating group connected to the forming azaallyl double bond is beneficial to β-H elimination. (4) The dissociation of the Ti–C bond and the addition of Ti–H are much less affected. However, the γ-H elimination requires more energy (16.3 *vs.* 14.4 kcal mol^{-1}), and the addition of Ti–H is more exergonic (19.5 *vs.* 17.8 kcal mol^{-1}). These differences can be ascribed to the more severe congestions in $\mathbf{TS10^{Et}–22^{Et}}$ and $\mathbf{13^{Et}}$ than in the corresponding $\mathbf{10^{Et}}$ and $\mathbf{14^{Et}}$. In addition, due to the stronger electron-donating capacity of the Et group, the electron-richer Ti centre in $\mathbf{22^{Et}}$ retards γ-H elimination. It is obvious that after the dispersion corrections, the β-H elimination reaction pathway to titanacycle $\mathbf{14^{Et}}$ requires an energy of 30.8 kcal mol^{-1}, the γ-H elimination reaction pathway has an energy barrier of 30.0 kcal mol^{-1}, and the system is exergonic by 12.3 kcal mol^{-1} with reference to $\mathbf{10^{Et}}$ [Fig. S6(c)†]. Compared to the case of $\mathbf{10^{Me}}$, formation of $\mathbf{14^{Et}}$ requires less apparent activation energy and has higher exergonicity. In contrast, the C–C coupling reaction pathway is kinetically more favourable for forming the diazatitanacyclopentane $\mathbf{25^{Et}}$. Compared to the case of **M9a**, in the C–C coupling reaction pathway, the elementary reactions require less energy, the breaking of Ti–C bond is less endergonic, and the C–C coupling is more exergonic. Herein, the fragmentation pathway of $\mathbf{27^{Et}}$, which includes β-H elimination, rotation of Cp*ClH segment, addition of Ti–H across azaallyl double bond, and other elementary

reaction steps was also explored, in order to obtain theoretical insights into the fragmentation of the analogues with other substituent groups. The calculated apparent activation energy barrier is more than 31 kcal mol^{-1} with reference to $\mathbf{10^{Et}}$ (Fig. S12†). As a consequence, the fragmentation of $\mathbf{27^{Et}}$ is unfavourable compared to that of $\mathbf{10^{Et}}$.

The energy barrier for the insertion of ArNC into the Ti–C bond is slightly reduced compared to that of EtNC (4.1 *vs.* 4.2 kcal mol^{-1}), which is ascribed to the fact that the conjugation with the Ar group stabilises the transition state of insertion. The formed $\mathbf{2^{Ar}}$ is a N-uncoordinated six-membered titanacycle. This is related to the reduced N-coordination ability of the ArNC moiety. The isomerisation of N-coordinated titanacycle $\mathbf{3^{Ar}}$ requires less energy (3.9 kcal mol^{-1}) and is less endergonic (1.4 kcal mol^{-1}) compared to the values calculated for *t*BuNC and MeNC. The C–C reductive elimination from $\mathbf{4^{Ar}}$ overcomes an energy barrier of 8.3 kcal mol^{-1} to form $\mathbf{5^{Ar}}$, and this step is exergonic by 7.9 kcal mol^{-1}. The required energy is less than those in the cases of *t*BuNC (11.5 kcal mol^{-1}), MeNC (9.3 kcal mol^{-1}), and EtNC (9.0 kcal mol^{-1}). The reduced activation energy barriers are related to the expanded conjugation of the π electrons in transition states. The insertion of ArNC into the Ti–H bond occurs rapidly to directly afford the N(ketimine)-coordinated $\mathbf{9^{Ar}}$, with the exergonicity of 7.9 kcal mol^{-1}. The direct formation of $\mathbf{9^{Ar}}$ is related to the more electron-deficient Ti centre for ArNC relative to *t*Bu and EtNC. The required energy for C–C reductive coupling is 1.8 kcal mol^{-1} higher than that of MeNC, and 1.0 kcal mol^{-1} lower than that of *t*BuNC. In the β-H elimination reaction pathway, the dissociation of Ti–N(ketimine) requires much less energy (1.1 kcal mol^{-1}) compared to the cases of *t*BuNC, MeNC, and EtNC. $\mathbf{11^{Ar}}$ is a stable intermediate due to π electron delocalisation. Subsequent β-H elimination directly leads to the formation of $\mathbf{20^{Ar}}$, overcoming the energy barrier of 16.3 kcal mol^{-1} and endergonic by 2.1 kcal mol^{-1}. $\mathbf{21^{Ar}}$ isomerises into $\mathbf{13^{Ar}}$, requiring more energy (13.1 kcal mol^{-1}) and being more endergonic (12.2 kcal mol^{-1}). The strong repulsion between the Cp* and Ar groups and the conjugation of system make the isomerisation difficult. The addition of the Ti–H bond requires 4.3 kcal mol^{-1} more energy in ArNC than in *t*BuNC, because the Ti–H bond is stronger in the case of ArNC. Similar to the cases of MeNC and EtNC, there is no agostic structure in the Ti–H bond addition product $\mathbf{14^{Ar}}$. Because π-electron delocalisation stabilises the transition state in the fragmentation of $\mathbf{14^{Ar}}$, this step requires less energy (14.0 kcal mol^{-1}) for ArNC than for *t*BuNC and MeNC. $\mathbf{TS22^{Ar}}$–$\mathbf{13^{Ar}}$, a transition state for γ-H elimination from $\mathbf{22^{Ar}}$, is higher in energy by 32.5 kcal mol^{-1} than $\mathbf{10^{Ar}}$, indicating that the γ-H elimination reaction pathway requires too much energy to occur. For the formation of the diazatitanacyclopentane $\mathbf{25^{Ar}}$, it can be found that the isomerisation reaction pathway is kinetically the most favourable, in which $\mathbf{9^{Ar}}$ isomerises into $\mathbf{26^{Ar}}$ with the endergonicity of 6.9 kcal mol^{-1}. The endergonicity is smaller than those in the cases of tBuNC, MeNC, and EtNC. The C–C reductive coupling requires 8.6 kcal mol^{-1} in energy and is much more exergonic for ArNC (16.1 kcal mol^{-1}) than for *t*BuNC (9.4 kcal mol^{-1}), MeNC (10.9 kcal mol^{-1}), and EtNC (11.7 kcal mol^{-1}). The insertion of C=N requires the energy of 13.0 kcal mol^{-1}, with the exergonicity of 4.6 kcal mol^{-1}. Apparently, for ArNC, after including the dispersion effects, the formation of α-methylene cyclopentenimine needs to overcome an energy barrier of 24.2 kcal mol^{-1} and is exergonic by 55.9 kcal mol^{-1} (Fig. S7 and S8†), and the formation of diazatitanacyclopentane requires 22.5 kcal mol^{-1} and is exergonic by 41.9 kcal mol^{-1} [Fig. S7–S9(b)†]. We theoretically predicted the possibility of generating a new "σ complex" ($\mathbf{25^{Ar}}$), because its formation is kinetically favourable. Experimentally, the diazahafnacyclopentane with the Ar groups has been observed and characterised by X-ray crystallography.[31] In $\mathbf{25^{Ar}}$, the lengths of Ti–C^7 (2.45 Å) and Ti–C^5 (2.49 Å) indicate that there is a C–C···Ti agostic interaction,[47] and the length of the C^7–C^5 bond (1.57 Å) is longer than those of C^7–C^1 and C^5–C^1 bonds (1.52 and 1.53 Å). The lengths of Ti–C^7 and Ti–C^5 are shorter than the reported lengths of the corresponding Hf–C (2.49 and 2.53 Å), and the C^7–C^5 bond is longer than the corresponding C–C bond (1.55 Å) in diazahafnacyclopentane.[31] These differences can be ascribed to the stronger C–C···Ti agostic interaction in diazatitanacyclopentane than that in the Hf counterpart. The calculated WBIs of Ti–C^7 and Ti–C^5 in $\mathbf{25^{Ar}}$ are 0.15 and 0.13, respectively, and the C–C···Ti interaction energy was calculated to be 44.8 kcal mol^{-1}.

The obtained conclusions for 1-AdNC are the same as those for *t*BuNC. From Fig. S10,† it can be inferred that considering the dispersion corrections, forming the bis-insertion product $\mathbf{10^{1\text{-}Ad}}$ requires an energy of 19.1 kcal mol^{-1} and is exergonic by 30.2 kcal mol^{-1}. In fact, $\mathbf{10^{1\text{-}Ad}}$ has been experimentally isolated.[31] The fragmentation of $\mathbf{10^{1\text{-}Ad}}$ into the Ti complex $\mathbf{18^{1\text{-}Ad}}$ and 1-Ad-substituted α-methylene cyclopentenimine $\mathbf{17^{1\text{-}Ad}}$ *via* the β-H elimination reaction pathway requires 27.7 kcal mol^{-1} and releases 11.9 kcal mol^{-1} in energy with reference to $\mathbf{10^{1\text{-}Ad}}$.

The mechanisms of the reactions of **M1a** with *t*BuNC, MeNC, EtNC, ArNC, and 1-AdNC are summarised in Scheme S2.† As shown in Scheme S2(a),† in the β-H reaction pathways for *t*BuNC and 1-AdNC, there are no intermediates like $\mathbf{19^R}$, $\mathbf{20^R}$, and $\mathbf{21^R}$ (R = Me and Et), because the bulky *t*Bu and 1-Ad groups hinder the rotation of the Cp*TiClH segment. The β-H elimination reaction pathway for ArNC does not produce intermediates like $\mathbf{12^{Me}}$ and $\mathbf{19^{Me}}$ for MeNC and $\mathbf{12^{Et}}$ and $\mathbf{19^{Et}}$ for EtNC. This is related to the combined effects of the bulkier ArNC moiety and its reduced N-coordination ability. The γ-H elimination reaction pathway for *t*BuNC, ArNC, and 1-AdNC is unfavourable, because the strong repulsion between the Cp* and *t*Bu, Ar, or 1-Ad group makes the transition state for γ-H elimination higher in energy. For ArNC, the formation of $\mathbf{25^{Ar}}$ (σ complex) *via* the isomerisation reaction pathway is favourable, due to the fact that the π electron delocalisation lowers the activation energy barrier of the reaction and stabilises the product $\mathbf{25^{Ar}}$.

Conclusions

The migratory insertion of isonitrile into metal–carbon bond is becoming a potentially important method for constructing C–C bonds in organic and pharmaceutical syntheses. In this work, we theoretically studied the reaction of Cp*(Cl)Ti(2,3-

dimethylbutadiene) with different isonitriles using DFT calculations. For *t*BuNC, MeNC, EtNC, ArNC, and 1-AdNC, the bis-insertion reaction of isonitrile all easily occurs at room temperature. After the dispersion corrections, the isomerisation of Cp*(Cl)Ti(2,3-dimethylbutadiene) determines the apparent activation energies of the bis-insertion reactions of the studied isonitriles, which is 19.1 kcal mol^{-1}. The bis-insertion reactions with the bulky *t*BuNC and 1-AdNC release less energy in comparison to those with the smaller MeNC and EtNC, and the exergonicity of the bis-insertion of electron-withdrawing ArNC is similar to that of the bulky *t*BuNC and 1-AdNC. The elementary reactions include isomerisation of Cp*(Cl)Ti(2,3-dimethylbutadiene), isonitrile coordination, isonitrile migratory insertion into the Ti–C and Ti–H bonds, isomerisation of six-membered titanacycle, C–C reductive elimination, β-H elimination, and C–C reductive coupling. The fused three-five metallabicyclic bis-insertion product titanaazidine can be experimentally observed, except that the product with the Ar groups is rapidly converted to diazatitanacyclopentane. In the presence of pyridine, the titanaazidines fragment into Ti imido complex and α-methylene cyclopentenimine for *t*BuNC, ArNC, and 1-AdNC. For isonitriles with bulky substitution groups such as *t*Bu and 1-Ad, the fragmentation of titanaazidines requires >27 kcal mol^{-1} and is exergonic by >11 kcal mol^{-1}. For the small MeNC and EtNC, considered the dispersion effects, the titanaazidines are converted to six-membered titanacycles, with a higher energy barrier of >30 kcal mol^{-1} and an exergonicity of <13 kcal mol^{-1}. In the case of ArNC, the fragmentation of titanaazidines requires the largest amount of energy (33.5 kcal mol^{-1}) and releases the largest amount of energy (24.7 kcal mol^{-1}), and the diazatitanacyclopentane with the Ar groups is an important intermediate. For the bulky *t*BuNC, ArNC, and 1-AdNC, the β-H elimination reaction pathway is responsible for the fragmentation of titanaazidines. The associated elementary reactions include dissociation of Ti–N(ketimine) bond, β-H elimination, isomerisation of Ti complex, addition of Ti–H bond, and fragmentation of titanacycle. For the small-sized MeNC and EtNC, the γ-H elimination reaction pathway competes with the β-H elimination reaction pathway. The former includes rotation of the Cp*TiClH segment and γ-H elimination. It is found that ArNC can be used to generate the diazatitanacyclopentane *via* the isomerisation reaction path, in which the system undergoes isomerisation of Ti complex, C–C reductive coupling, and insertion of the C=N bond. The results presented here are expected to be useful for chemists to synthesise new substances *via* the reaction of Ti complex and isonitriles. A theoretical study of the reaction of Cp*(Cl)Hf(diene) with isonitriles is underway.

Conflicts of interest

There are no conflicts of interest to declare.

Acknowledgements

We are grateful for the financial support from The Natural Sciences Foundation of Anhui Province (1608085MB42), Scientific Research Foundation of Anhui University of Science and Technology (ZY538), Beijing National Laboratory for Molecular Sciences (1G129), and The Undergraduate Innovation and Entrepreneurship Training Program (201610361242). We thank professors Song Wang and Zhao Xi at Jilin University (JLU) for calculation resource support.

Notes and references

1 (*a*) A. L. dom and T. J. McDaniel, *Acc. Chem. Res.*, 2015, **48**, 2822–2833; (*b*) J. Majer, P. Kwiatkowski and J. Jurczak, *Org. Lett.*, 2011, **13**, 5944–5947; (*c*) A. Millán, L. Á. De Cienfuegos, D. Miguel, A. G. Campaña and J. M. Cuerva, *Org. Lett.*, 2012, **14**, 5984–5987; (*d*) Z. W. Davis-Gilbert, L. J. Yao and I. A. Tonks, *J. Am. Chem. Soc.*, 2016, **138**, 14570–14573; (*e*) B. Wu, M. W. Bezpalko, B. B. Foxman and C. M. Thomas, *Chem. Sci.*, 2016, **6**, 2044–2049.

2 (*a*) Z. Chen, J. Liu, H. Pei, W. Liu, Y. Chen, J. Wu, W. Li and Y. Li, *Org. Lett.*, 2015, **17**, 3406–3409; (*b*) C.-C. Chang, F. Jin, L.-Y. Jang, J.-F. Lee and S. Cheng, *Catal. Sci. Technol.*, 2016, **6**, 7631–7642; (*c*) H. Shen, Y. Wang and Z. Xie, *Org. Lett.*, 2011, **13**, 4562–4565; (*d*) D. Hollmann, K. Grabow, J. Jiao, M. Kessler, A. Spannenberg, T. Beweries, U. Bentrup and A. Brückner, *Chem.–Eur. J.*, 2013, **19**, 13705–13713; (*e*) J. A. Suttil and D. S. McGuinness, *Organometallics*, 2012, **31**, 7004–7010.

3 (*a*) A. Rosales, J. Muñoz-Bascón, C. López-Sánchez, M. Álvarez-Corral, M. Muñoz-Dorado, I. Rodríguez-García and J. E. Oltra, *J. Org. Chem.*, 2012, **77**, 4171–4176; (*b*) L. Becker, P. Arndt, A. Spannenberg, H. Jiao and U. Rosenthal, *Angew. Chem.*, 2015, **127**, 5614–5617; (*c*) I. R. Márquez, D. Miguel, A. Millán, M. L. Marcos and L. Á. de Cienfuegos, *J. Org. Chem.*, 2014, **79**, 1529–1541; (*d*) Z. Chen, J. Wu, Y. Chen, L. Li, Y. Xia, Y. Li, W. Liu, T. Lei, L. Yang, D. Gao and W. Li, *Organometallics*, 2012, **31**, 6005–6013; (*e*) H. A. Spinney, C. R. Clough and C. C. Cummins, *Dalton Trans.*, 2015, **44**, 6784–6796.

4 (*a*) Q. L. Lu, Q. Q. Luo, Y. D. Li and S. G. Huang, *Phys. Chem. Chem. Phys.*, 2015, **17**, 20897–20902; (*b*) M. Sumimoto, Y. Kawashima, K. Hori and H. Fujimoto, *Phys. Chem. Chem. Phys.*, 2015, **17**, 6478–6483; (*c*) A. D. Schwarz, A. Nova, E. Clot and P. Mountford, *Chem. Commun.*, 2011, **47**, 4926–4928; (*d*) A. C. Behrle, J. R. Levin, J. E. Kim, J. M. Drewett, C. L. Barnes, E. J. Schelter and J. R. Walensky, *Dalton Trans.*, 2015, **44**, 2693–2702; (*e*) T. A. Manz, *RSC Adv.*, 2015, **5**, 48246–48254.

5 (*a*) R. Robinson, D. S. McGuinness and B. F. Yates, *ACS Catal.*, 2013, **3**, 3006–3015; (*b*) P. J. Tiong, A. Nova, L. R. Groom, A. D. Schwarz, J. D. Selby, A. D. Schofield, E. Clot and P. Mountford, *Organometallics*, 2011, **30**, 1182–1201; (*c*) A. D. Schofield, A. Nova, J. D. Selby, A. D. Schwarz, E. Clot and P. Mountford, *Chem.–Eur. J.*, 2011, **17**, 265–285; (*d*) C. Prieto, J. A. G. Delgado, J. F. Arteaga, M. Jaraíz, J. L. López-Pérez and A. F. Barrero, *Org. Biomol. Chem.*, 2015, **3**, 3462–3469; (*e*) K. Nomura, S. Patamma, H. Matsuda, S. Katao, K. Tsutsumi and H. Fukuda, *RSC Adv.*, 2015, **5**, 64503–64513.

6 (*a*) K. Kim, S. H. Choi, D. Ahn, Y. Kim, J. Y. Ryu, J. Lee and Y. Kim, *RSC Adv.*, 2016, **6**, 97800–97807; (*b*) S. Basu, P. S. Kandiyal, R. S. Ampapathway and T. K. Chakraborty, *RSC Adv.*, 2013, **3**, 13630–13634; (*c*) D. A. Smith and O. V. Ozerov, *Chem. Commun.*, 2011, **47**, 10779–10781; (*d*) C. Paniagua, M. E. G. Mosquera, T. Cuenca and G. Jiménez, *Organometallics*, 2011, **30**, 2993–3000; (*e*) A. C. T. Kuate, S. K. Mohapatra, C. G. Daniliuc, P. G. Jones and M. Tamm, *Organometallics*, 2012, **31**, 8544–8555.

7 (*a*) A. Millán, A. Martín-Lasanta, D. Miguel, L. Á. de Cienfuegos and J. M. Cuerva, *Chem. Commun.*, 2011, **47**, 10470–10472; (*b*) J. A. Sutti, M. F. Shaw, D. S. McGuinness, M. G. Gardiner and S. J. Evans, *Dalton Trans.*, 2013, **42**, 9129–9138; (*c*) A. Rosales, J. Muñoz-Bascón, V. M. Morales-Alcázar, J. A. Castilla-Alcalá and J. E. Oltra, *RSC Adv.*, 2012, **2**, 12922–12925; (*d*) M. Lein, J. A. Harrison and A. J. Nielson, *Dalton Trans.*, 2011, **40**, 10731–10741.

8 (*a*) G. B. Wijeratne, E. M. Zolnhofer, S. Fortier, L. N. Grant, P. J. Carroll, C.-H. Chen, K. Meyer, J. Krzystek, A. Ozarowski, T. A. Jackson, D. J. Mindiola and J. Telser, *Inorg. Chem.*, 2015, **54**, 10380–10397; (*b*) M. Kessler, S. Hansen, D. Hollmann, M. Klahn, T. Beweries, A. Spannenberg, A. Brückner and U. Rosenthal, *Eur. J. Inorg. Chem.*, 2011, 627–631; (*c*) C. Adler, N. Frerichs, M. Schmidtmann and R. Beckhaus, *Organometallics*, 2016, **35**, 3728–3733; (*d*) A. F. R. Kilpatrick, J. C. Green and F. G. N. Cloke, *Organometallics*, 2015, **34**, 4816–4829.

9 (*a*) K. Kaleta, M. Kessler, T. Beweries, P. Arndt, A. Spannenberg and U. Rosenthal, *Eur. J. Inorg. Chem.*, 2011, 3388–3393; (*b*) A. F. Dunlop-Brière, M. C. Baird and P. H. M. Budzelaar, *Organometallics*, 2015, **34**, 5245–5253; (*c*) F. Hermant, E. Urbańska, S. S. de Mazancourt, T. Maubert, E. Nicolas and Y. Six, *Organometallics*, 2014, **33**, 5643–5653; (*d*) Y. Takii, P. M. Gurubasavaraj, S. Katao and K. Nomura, *Organometallics*, 2012, **31**, 8237–8248.

10 (*a*) X. Wang, Y. Wang, S. Li, Y. Zhang and P. Ma, *J. Phys. Chem. A*, 2016, **120**, 5457–5463; (*b*) P. J. Tiong, A. Nova, E. Clot and P. Mountford, *Chem. Commun.*, 2011, **47**, 3147–3149; (*c*) P. J. Tiong, A. Nova, A. D. Schwarz, J. D. Selby, E. Clot and P. Mountford, *Dalton Trans.*, 2012, **41**, 2277–2288; (*d*) K. Altenburger, F. Reiβ, K. Schubert, W. Baumann, A. Spannenberg, P. Arndt and U. Rosenthal, *Eur. J. Inorg. Chem.*, 2015, 1709–1715.

11 (*a*) A. M. Chapman and D. F. Wass, *Dalton Trans.*, 2012, **41**, 9067–9072; (*b*) P. González-Navarrete, M. Calatayud, J. Andrés, F. Ruipérez and D. Roca-Sanjuán, *J. Phys. Chem. A*, 2013, **117**, 5354–5364; (*c*) A. V. Chuchuryukin, R. Huang, M. Lutz, J. C. Chadwick, A. L. Spek and G. van Koten, *Organometallics*, 2011, **30**, 2819–2830; (*d*) T. Miyazaki, Y. Tanabe, M. Yuki, Y. Miyake and Y. Nishibayashi, *Organometallics*, 2011, **30**, 3195–3199.

12 (*a*) S. K. Guchhait, V. Chaudhary and C. Madaan, *Org. Biomol. Chem.*, 2012, **10**, 9271–9277; (*b*) W. Sha, J.-T. Yu, Y. Jiang, H. Yang and J. Cheng, *Chem. Commun.*, 2014, **50**, 9179–9181; (*c*) Y. Li, A. Chao and F. F. Fleming, *Chem. Commun.*, 2016, **52**, 2111–2113; (*d*) G. Lesma, I. Bassanini, R. Bortolozzi, C. Colletto, R. Bai, E. Hamel, F. Meneghetti, G. Rainoldi, M. Stucchi, A. Sacchetti, A. Silvani and G. Viola, *Org. Biomol. Chem.*, 2015, **13**, 11633–11644; (*e*) M. Tobisu and N. Chatani, *Chem. Lett.*, 2011, **40**, 330–340.

13 (*a*) T. Buyck, D. Pasche, Q. Wang and J. Zhu, *Chem.–Eur. J.*, 2016, **22**, 2278–2281; (*b*) B. Zhang and A. Studer, *Org. Lett.*, 2014, **16**, 1216–1219; (*c*) B. Zhang and A. Studer, *Org. Lett.*, 2014, **16**, 3990–3993; (*d*) Q. Dai, J.-T. Yu, X. Feng, Y. Jiang, H. Yang and J. Cheng, *Adv. Synth. Catal.*, 2014, **356**, 3341–3346.

14 (*a*) A. Dewanji, C. Mück-Lichtenfeld, K. Bergander, C. G. Daniliuc and A. Studer, *Chem.–Eur. J.*, 2015, **21**, 12295–12298; (*b*) A. Hinz, A. Schulz and A. Villinger, *J. Am. Chem. Soc.*, 2015, **137**, 9953–9962; (*c*) N. Shao, G.-X. Pang, C.-X. Yan, G.-F. Shi and Y. Cheng, *J. Org. Chem.*, 2011, **76**, 7458–7465; (*d*) S. U. Dighe, A. K. K. S., S. Srivastava, P. Shukla, S. Singh, M. Dikshit and S. Batra, *J. Org. Chem.*, 2015, **80**, 99–108.

15 (*a*) Y. Li and F. F. Fleming, *Angew. Chem., Int. Ed.*, 2016, **55**, 14770–14773; (*b*) D. Riedel, T. Wurm, K. Graf, M. Rudolph, F. Rominger and A. S. K. Hashmi, *Adv. Synth. Catal.*, 2015, **357**, 1515–1523; (*c*) M. Seidl, M. Schiffer, M. Bodensteiner, A. Y. Timoshkin and M. Scheer, *Chem.–Eur. J.*, 2013, **19**, 13787–13791; (*d*) S. Tong, Q. Wang, M.-X. Wang and J. Zhu, *Angew. Chem., Int. Ed.*, 2015, **54**, 1293–1297.

16 (*a*) S. Tong, Q. Wang, M.-X. Wang and J. Zhu, *Chem.–Eur. J.*, 2016, **22**, 8332–8338; (*b*) R. M. Wilson, J. L. Stockdill, X. Wu, X. Li, P. A. Vadola, P. K. Park, P. Wang and S. J. Danishefsky, *Angew. Chem., Int. Ed.*, 2012, **51**, 2834–2848; (*c*) B. Zhang, C. Mück-Lichtenfeld, C. G. Daniliuc and A. Studer, *Angew. Chem., Int. Ed.*, 2013, **52**, 10792–10795; (*d*) A. S. K. Hashmi, C. Lothschütz, C. Böhling and F. Rominger, *Organometallics*, 2011, **30**, 2411–2417.

17 (*a*) H. Zhang, D. Shi, S. Ren, H. Jin and Y. Liu, *Eur. J. Org. Chem.*, 2016, 4224–4229; (*b*) R. S. Chay, K. V. Luzyanin, V. Y. Kukushkin, M. F. C. G. da Silva and A. J. L. Pombeiro, *Organometallics*, 2012, **31**, 2379–2387; (*c*) H. V. Le and B. Ganem, *Org. Lett.*, 2011, **13**, 2584–2585; (*d*) M. Maj, C. Ahn, D. Kossowska, K. Park, K. Kwak, H. Han and M. Cho, *Phys. Chem. Chem. Phys.*, 2015, **17**, 11770–11778.

18 (*a*) M. Adib, S. Feizi, M. S. Shirazi, L.-G. Zhu and H. R. Bijanzadeh, *Helv. Chim. Acta*, 2014, **97**, 524–531; (*b*) H. Stöckmann, A. A. Neves, S. Stairs, K. M. Brindle and F. J. Leeper, *Org. Biomol. Chem.*, 2011, **9**, 7303–7305; (*c*) G. Bianchini, G. L. Sorella, N. Canever, A. Scarso and G. Strukul, *Chem. Commun.*, 2013, **49**, 5322–5324.

19 (*a*) E. Vitaku, D. T. Smith and J. T. Njardarson, *J. Med. Chem.*, 2014, **57**, 10257–10274; (*b*) S. D. Roughley and A. M. Jordan, *J. Med. Chem.*, 2011, **54**, 3451–3479; (*c*) J. S. Carey, D. Laffan, C. Thomson and M. T. Williams, *Org. Biomol. Chem.*, 2006, **4**, 2337–2347.

20 (*a*) D. M. Stout and A. I. Meyers, *Chem. Rev.*, 1982, **82**, 223–243; (*b*) R. Lavilla, *J. Chem. Soc., Perkin Trans. 1*, 2002, 141–1156; (*c*) J. A. Bull, J. J. Mousseau, G. Pelletier and A. B. Charette, *Chem. Rev.*, 2012, **112**, 2642–2713.

21 (*a*) A. Molnár, *Chem. Rev.*, 2011, **111**, 2251–2320; (*b*) T. J. Colacot and J. Matthey, *Platinum Met. Rev.*, 2011, **55**, 84–90; (*c*) C. Beemelmanns and H.-U. Reissig, *Chem. Soc.*

Rev., 2011, **40**, 2199–2210; (*d*) C. S. Yeung and V. M. Dong, *Chem. Rev.*, 2011, **111**, 1215–1292; (*e*) T. Ahrens, J. Kohlmann, M. Ahrens and T. Braun, *Chem. Rev.*, 2015, **115**, 931–972.

22 (*a*) A. A. O. Sarhan and C. Bolm, *Chem. Soc. Rev.*, 2009, **38**, 2730–2744; (*b*) F. Monnier and M. Taillefer, *Angew. Chem., Int. Ed.*, 2009, **48**, 6954–6971; (*c*) L. Yin and J. Liebscher, *Chem. Rev.*, 2007, **107**, 133–173; (*d*) J.-P. Corbet and G. Mignani, *Chem. Rev.*, 2006, **106**, 2651–2710.

23 (*a*) D. A. Colby, R. G. Bergman and J. A. Ellman, *Chem. Rev.*, 2010, **110**, 624–655; (*b*) L. Souillart and N. Cramer, *Chem. Rev.*, 2015, **115**, 9410–9464; (*c*) M. Shibasaki and M. Kanai, *Chem. Rev.*, 2008, **108**, 2852–2873; (*d*) E. M. Beccalli, G. Broggini, M. Martinelli and S. Sottocornola, *Chem. Rev.*, 2007, **107**, 5318–5365.

24 (*a*) N. M. G. Franssen, A. J. C. Walters, J. N. H. Reek and B. de Bruin, *Catal. Sci. Technol.*, 2011, **1**, 153–165; (*b*) S. G. Modha, V. P. Mehta and E. V. Van der Eycken, *Chem. Soc. Rev.*, 2013, **42**, 5042–5055; (*c*) R. Kumar and E. V. Van der Eycken, *Chem. Soc. Rev.*, 2013, **42**, 1121–1146; (*d*) W. Shi, C. Liu and A. Lei, *Chem. Soc. Rev.*, 2011, **40**, 2761–2776.

25 (*a*) K. Huang, C.-L. Sun and Z.-J. Shi, *Chem. Soc. Rev.*, 2011, **40**, 2435–2452; (*b*) A. P. Thankachan, S. Asha, K. S. Sindhu and G. Anilkumar, *RSC Adv.*, 2015, **5**, 62179–62193; (*c*) J. Legros and B. Figadère, *Nat. Prod. Rep.*, 2015, **32**, 1541–1555; (*d*) U. Schneider and S. Kobayashi, *Acc. Chem. Res.*, 2012, **45**, 1331–1344.

26 (*a*) A. Zeiler, M. Rudolph, F. Rominger and A. S. K. Hashmi, *Chem.–Eur. J.*, 2015, **21**, 11065–11071; (*b*) G. Pendecy and S. Batra, *RSC Adv.*, 2015, **5**, 28875–28878; (*c*) H. Gu, Z. Qiu, Z. Zhang, J. Li and B. Yan, *Dalton Trans.*, 2015, **44**, 9839–9846; (*d*) H. Jiang, H. Gao, B. Liu and W. Wu, *Chem. Commun.*, 2004, **50**, 15348–15351.

27 (*a*) L. Xiang and Z. Xie, *Organometallics*, 2016, **35**, 233–241; (*b*) L. Xiang and Z. Xie, *Organometallics*, 2016, **35**, 1430–1439; (*c*) K. Takamatsu, K. Hirano and M. Miura, *Org. Lett.*, 2015, **17**, 4066–4069; (*d*) T. N. Valadez, J. R. Norton, M. C. Neary and P. J. Quinlivan, *Organometallics*, 2016, **35**, 3163–3169.

28 (*a*) F. Foschi, T. Roth, H. Wadepohl and L. H. Gade, *Org. Lett.*, 2016, **18**, 5182–5185; (*b*) H. Braunschweig, M. A. Celik, R. D. Dewhurst, K. Ferkinghoff, A. Hermann, J. O. C. Jimenez-Halla, T. Kramer, K. Radacki, R. Shang, E. Siedler, F. Weißenberger and C. Werner, *Chem.–Eur. J.*, 2016, **22**, 11736–11744; (*c*) C.-H. Lei, D.-X. Wang, L. Zhao, J. Zhu and M.-X. Wang, *J. Am. Chem. Soc.*, 2013, **135**, 4708–4711; (*d*) W. Lu, H. Lu, Y. Li, R. Ganguly and R. Kinjo, *J. Am. Chem. Soc.*, 2016, **138**, 6650–6661.

29 (*a*) H.-Y. Tu, Y.-R. Liu, J.-J. Chu, B.-L. Hu and X.-G. Zhang, *J. Org. Chem.*, 2014, **79**, 9907–9912; (*b*) M. Ma, A. Stasch and C. Jones, *Chem.–Eur. J.*, 2012, **18**, 10669–10676; (*c*) Y. Odabachian, S. Tong, Q. Wang, M.-X. Wang and J. Zhu, *Angew. Chem., Int. Ed.*, 2013, **52**, 10878–10828; (*d*) A. G. Tskhovrebov, K. V. Luzyanin, F. M. Dolgushin, M. F. C. G. da Silva, A. J. L. Pombeiro and V. Y. Kukushkin, *Organometallics*, 2011, **30**, 3362–3370; (*e*) M. Okazaki, K. Suto, N. Kudo, M. Takano and F. Ozawa, *Organometallics*, 2012, **31**, 4110–4113.

30 G. Greidanus-Strom, C. A. G. Carter and J. M. Stryker, *Organometallics*, 2002, **21**, 1011–1013.

31 T. N. Valadez, J. R. Norton and M. C. Neary, *J. Am. Chem. Soc.*, 2015, **137**, 10152–10155.

32 (*a*) M. J. Frisch, G. W. Trucks, H. B. Schlegel, G. E. Scuseria, M. A. Robb, J. R. Cheeseman, G. Scalmani, V. Barone, B. Mennucci, G. A. Petersson, H. Nakatsuji, M. Caricato, X. Li, H. P. Hratchian, A. F. Izmaylov, J. Bloino, G. Zheng, J. L. Sonnenberg, M. Hada, M. Ehara, K. Toyota, R. Fukuda, J. Hasegawa, M. Ishida, T. Nakajima, Y. Honda, O. Kitao, H. Nakai, T. Vreven, J. A. Montgomery Jr, J. E. Peralta, F. Ogliaro, M. Bearpark, J. J. Heyd, E. Brothers, K. N. Kudin, V. N. Staroverov, R. Kobayashi, J. Normand, K. Raghavachari, A. Rendell, J. C. Burant, S. S. Iyengar, J. Tomasi, M. Cossi, N. Rega, J. M. Millam, M. Klene, J. E. Knox, J. B. Cross, V. Bakken, C. Adamo, J. Jaramillo, R. Gomperts, R. E. Stratmann, O. Yazyev, A. J. Austin, R. Cammi, C. Pomelli, J. W. Ochterski, R. L. Martin, K. Morokuma, V. G. Zakrzewski, G. A. Voth, P. Salvador, J. J. Dannenberg, S. Dapprich, A. D. Daniels, O. Farkas, J. B. Foresman, J. V. Ortiz, J. Cioslowski and D. J. Fox, *Gaussian 09 Revision A.02*, Gaussian, Inc., Wallingford CT, 2009; (*b*) M. J. Frisch, G. W. Trucks, H. B. Schlegel, G. E. Scuseria, M. A. Robb, J. R. Cheeseman, G. Scalmani, V. Barone, B. Mennucci, G. A. Petersson, H. Nakatsuji, M. Caricato, X. Li, H. P. Hratchian, A. F. Izmaylov, J. Bloino, G. Zheng, J. L. Sonnenberg, M. Hada, M. Ehara, K. Toyota, R. Fukuda, J. Hasegawa, M. Ishida, T. Nakajima, Y. Honda, O. Kitao, H. Nakai, T. Vreven, J. A. Montgomery Jr, J. E. Peralta, F. Ogliaro, M. Bearpark, J. J. Heyd, E. Brothers, K. N. Kudin, V. N. Staroverov, T. Keith, R. Kobayashi, J. Normand, K. Raghavachari, A. Rendell, J. C. Burant, S. S. Iyengar, J. Tomasi, M. Cossi, N. Rega, J. M. Millam, M. Klene, J. E. Knox, J. B. Cross, V. Bakken, C. Adamo, J. Jaramillo, R. Gomperts, R. E. Stratmann, O. Yazyev, A. J. Austin, R. Cammi, C. Pomelli, J. W. Ochterski, R. L. Martin, K. Morokuma, V. G. Zakrzewski, G. A. Voth, P. Salvador, J. J. Dannenberg, S. Dapprich, A. D. Daniels, O. Farkas, J. B. Foresman, J. V. Ortiz, J. Cioslowski and D. J. Fox, *Gaussian 09, Revision E.01*, Gaussian, Inc., Wallingford CT, 2013.

33 A. D. Becke, *J. Chem. Phys.*, 1993, **98**, 5648–5652.

34 C. Lee, W. Yang and R. G. Parr, *Phys. Rev. B: Condens. Matter Mater. Phys.*, 1988, **37**, 785–789.

35 J. Tomasi, B. Mennucci and R. Cammi, *Chem. Rev.*, 2005, **105**, 2999–3094.

36 P. J. Hay and W. R. Wadt, *J. Chem. Phys.*, 1985, **82**, 270–283.

37 W. R. Wadt and P. J. Hay, *J. Chem. Phys.*, 1985, **83**, 284–298.

38 A. W. Ehlers, M. Böhme, S. Dapprich, A. Gobbi, A. Höllwarth, V. Jonas, K. F. Köhler, R. Stegmann, A. Veldkamp and G. Frenking, *Chem. Phys. Lett.*, 1993, **208**, 111–114.

39 A. Höllwarth, M. Böhme, S. Dapprich, A. W. Ehlers, A. Gobbi, V. Jonas, K. F. Köhler, R. Stegmann, A. Veldkamp and G. Frenking, *Chem. Phys. Lett.*, 1993, **82**, 237–240.

40 P. J. Hay and W. R. Wadt, *J. Chem. Phys.*, 1985, **82**, 299–310.
41 W. J. Hehre, R. Ditchfield and J. A. Pople, *J. Chem. Phys.*, 1972, **56**, 2257–2261.
42 R. Krishnan, J. S. Binkley, R. Seeger and J. A. Pople, *J. Chem. Phys.*, 1972, **72**, 650–654.
43 V. A. Rassolov, M. A. Ratner, J. A. Pople, P. C. Redfern and L. A. Curtiss, *J. Comput. Chem.*, 2011, **22**, 976–984.
44 (*a*) C. Gonzalez and H. B. Schlegel, *J. Chem. Phys.*, 1989, **90**, 2154–2161; (*b*) C. Gonzalez and H. B. Schlegel, *J. Phys. Chem.*, 1990, **94**, 5523–5527.
45 (*a*) R. Sperger, I. A. Sanhueza, I. Kalvet and F. Schoenebeck, *Chem. Rev.*, 2015, **115**, 9532–9586; (*b*) V. Singh, Y. Nakao, S. Sakaki and M. M. Deshmukh, *J. Org. Chem.*, 2017, **82**, 289–301.
46 L. R. Groom, A. D. Schwarz, A. Nova, E. Clot and P. Mountford, *Organometallics*, 2013, **32**, 7520–7539.
47 M. Etienne and A. S. Weller, *Chem. Soc. Rev.*, 2014, **43**, 242–259.